Computing, Telecommunication and Control, 2025, Vol. 18, No. 3, Pp. 111–122.
Информатика, телекоммуникации и управление. 2025. Том 18, № 3. С. 111–122.

Research article
DOI: https://doi.org/10.18721/JCSTCS.18310
UDC 621.372.8

TOPOLOGY AND DESIGN METHODOLOGY OF A QUADRATURE WAVEGUIDE POWER DIVIDER FOR AN ARBITRARY FREQUENCY RANGE

D.V. Lomsadze, N.G. Kolmakova, S.V. Volvenko ✉

Peter the Great St. Petersburg Polytechnic University,
St. Petersburg, Russian Federation

✉ volk@cee.spbstu.ru

Abstract. This article focuses on the modeling of a quadrature waveguide power divider, taking into account technological requirements and manufacturing feasibility. A relatively simple yet effective device topology is proposed, along with a method for calculating its geometric parameters to operate reliably within a predefined frequency range. The study includes a comprehensive analysis of existing power divider configurations, provides a detailed overview of the theoretical foundations for designing a quadrature waveguide-slot bridge and an in-depth examination of all design stages of the power divider, using the 27–35 GHz frequency range as an example. Based on the developed model, a working prototype was fabricated. Measurements of its frequency characteristics confirmed the validity and practical applicability of the proposed approach. The design methodology developed in this work can be effectively applied to create a quadrature waveguide-slot bridge in any given frequency range, making it a versatile tool for engineers and researchers in the field of microwave technologies.

Keywords: quadrature power divider, waveguide-slot bridge, rectangular waveguide, calculation method, device topology

Citation: Lomsadze D.V., Kolmakova N.G., Volvenko S.V. Topology and design methodology of a quadrature waveguide power divider for an arbitrary frequency range. Computing, Telecommunications and Control, 2025, Vol. 18, No. 3, Pp. 111–122. DOI: 10.18721/JCSTCS.18310

Научная статья
DOI: https://doi.org/10.18721/JCSTCS.18310
УДК 621.372.8

ТОПОЛОГИЯ И МЕТОДИКА ПРОЕКТИРОВАНИЯ КВАДРАТУРНОГО ВОЛНОВОДНОГО ДЕЛИТЕЛЯ МОЩНОСТИ ДЛЯ ПРОИЗВОЛЬНОГО ДИАПАЗОНА ЧАСТОТ

Д.В. Ломсадзе, Н.Г. Колмакова, С.В. Волвенко ✉

Санкт-Петербургский политехнический университет Петра Великого,
Санкт-Петербург, Российская Федерация

✉ volk@cee.spbstu.ru

Аннотация. Данная статья посвящена моделированию квадратурного волноводного делителя мощности с учетом технологических требований и возможностей его изготовления. Предложена довольно простая, но эффективная топология устройства, а также методика расчета его геометрических параметров для обеспечения надежной работы в предварительно заданном частотном диапазоне. В работе представлен комплексный анализ существующих конфигураций делителей мощности, дан подробный обзор теоретических основ проектирования квадратурного волноводно-щелевого моста, а также детально рассмотрены все этапы проектирования делителя мощности на примере частотного диапазона 27–35 ГГц. На основе разработанной методики получена модель, благодаря которой был изготовлен рабочий опытный образец квадратурного волноводно-щелевого моста. Результаты измерения его частотных характеристик подтвердили корректность и обоснованность предложенного подхода, а также его практическую применимость. Разработанная в рамках данной работы методика проектирования может быть эффективно применена для создания квадратурного волноводно-щелевого моста в любом заданном диапазоне частот, что делает ее универсальным инструментом для инженеров и исследователей в области СВЧ-технологий.

Ключевые слова: квадратурный делитель мощности, волноводно-щелевой мост, прямоугольный волновод, методика расчета, топология устройства

Для цитирования: Lomsadze D.V., Kolmakova N.G., Volvenko S.V. Topology and design methodology of a quadrature waveguide power divider for an arbitrary frequency range // Computing, Telecommunications and Control. 2025. Т. 18, № 3. С. 111–122. DOI: 10.18721/JCSTCS.18310

Introduction

Power dividers (PD) are essential components of modern microwave technology. They are widely used in power amplifiers [1], antenna arrays [2] and other transceivers [3]. Advances in technology and production capabilities, along with the demand for wider communication channels and the increasing number of electronic devices, have driven interest in PDs operating at frequencies above 10 GHz. This trend requires efficient broadband signal processing and transmission, which can be achieved using various types of transmission lines. These include fiber-optic links [4], dielectric waveguides based on low-density polyethylene [5] and traditional hollow metallic waveguides. Each of these technologies offers distinct advantages in terms of size, weight, loss characteristics and ease of integration. However, hollow metallic waveguides possess the unique ability to handle high microwave power levels without significant losses or electrical breakdown, making them the primary choice for high-power applications, particularly in radar and satellite systems. Another option is to use microstrip and other planar structures; however, they suffer from increased dielectric and conductor losses at high frequencies [6], which

further reinforces the need for low-loss, high-power-capable waveguide solutions[1]. The most common PDs are those that split the input power equally between two output channels. These are T-, E- and Y-junctions [7, 8], double waveguide tees or magic tee [9], waveguide-slot bridges [10] and others. Depending on the type of junction, the output ports may be in-phase, out-of-phase or exhibit a 90° phase difference. Cascading of such PD [11] makes it possible to design a divider with a large number of output channels. Quadrature PDs stand out among these structures, with quadrature waveguide-slot bridges (QWSB) being one of their representatives. QWSB are four-channel devices that provide an equal power division between two output channels with a 90° phase shift. Their key advantage is the ability to terminate the remaining output with a load, ensuring isolation between the two power-divided output channels. The optimal behavior of QWSB is achieved either by selecting a special complex geometry of the matching area [10] or by using various matching elements such as inductive posts[2] and resistive baffles [12], which further complicate the configuration of the device.

The literature describes several techniques for designing waveguide-slot bridges by selecting a special geometry. For example, [13] considers a step transition as the matching section. However, this approach is highly sensitive to manufacturing tolerances and complicates fabrication, particularly at high frequencies. A solution to this issue was proposed in [10], where the step transition in the matching region is replaced with a smooth bend, reducing manufacturing complexity. However, the authors of this article do not pay enough attention to explaining the synthesis of the geometry of the PD.

To fill this gap, this paper provides a detailed method for designing a quadrature PD within a predefined frequency range without using complex geometries or extra elements. The capabilities of the proposed topology and its design methodology are demonstrated through the development of a broadband quadrature PD in the 27–35 GHz frequency range.

Concept and design of a quadrature PD for a predefined frequency range

This paper presents a design technique for an H-plane QWSB. It demonstrates how power division can be achieved within a given frequency range by selecting appropriate geometric parameters of the proposed topology. This approach is applicable to various frequency ranges and is limited only by the allowable range of changes in the geometric parameters of the structure. Fig. 1 shows the geometry of the PD being developed along with the key geometric parameters.

To design a quadrature PD in the frequency range (f_0, f_1) the following steps are necessary:

1. Select the appropriate cross-sectional dimensions of the rectangular waveguides a and b.
2. Use a simplified theoretical model to estimate the initial approximations of the main parameters of the splitting region d and L.
3. Based on the technological requirements and manufacturing capabilities, determine the minimum allowable value of e.
4. Set initial approximations for the parameters s and n.
5. Use an optimization process to determine the geometric parameters that provide the best matching and require division within the frequency band.

Let us look at these steps in more detail.

1. First, the dimensions of the rectangular waveguide must be selected such that the specified frequency range (f_0, f_1) lies within the operating range of this waveguide. From a practical point of view, rectangular waveguides of standard dimensions are the most convenient. However, a choice of non-standard waveguide sizes is also possible.

2. To estimate the initial approximations of parameters d and L, consider an ideal model of the waveguide-slot bridge[3], which consists of two waveguides connected along a narrow wall (shaded area

[1] Murav'ev V.V., Korenevskii S.A., Mishchenko V.N. Sverkhvysokochastotnye tekhnologii v sistemakh telekommunikatsii [Ultra-high-frequency technologies in telecommunication systems]. Minsk: BGUIR, 2007.
[2] Vol'man V.I., Pimenov Iu.V. Tekhnicheskaia elektrodinamika [Technical electrodynamics]. Moscow: Sviaz', 1971.
[3] Vol'man V.I., Pimenov Iu.V. Tekhnicheskaia elektrodinamika [Technical electrodynamics]. Moscow: Sviaz', 1971.

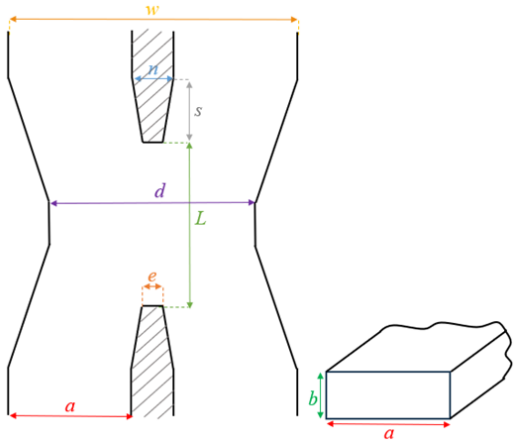

Fig. 1. Geometry of the H-plane PD with key parameters

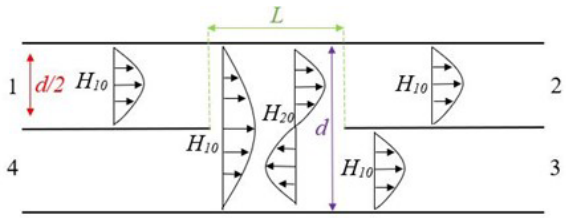

Fig. 2. The principle of operation of the waveguide-slot bridge

in Fig. 1). In this case, the width of the feeding waveguides is half the width of the splitting region, i.e., $d/2$. Channel 1 is excited by the H_{10} mode, while channels 2 and 3 are output channels where H_{10} modes with half amplitude and 90° phase shift propagate, and channel 4 has to be isolated. The absence of a propagating H_{10} mode in channel 4 is possible as a result of the combination of two H_{10} modes of equal amplitude and a phase difference of 180°, while all feeding waveguides must operate in the single-mode range. Thus, the problem can be considered as the sum of two cases: in the first case ports 1 and 4 are simultaneously excited in-phase, and in the second case they are excited in antiphase.

Assume that only H_{10} and H_{20} modes of the rectangular waveguide with width d can propagate in the splitting region, that is $f_1 < f_{H30}$, where f_{H30} is the cutoff frequency for H_{30} mode of the rectangular waveguide with width d. Since the feeding waveguides are single-mode, we can deduct from the definition of the cutoff frequency that

$$\frac{c}{f_0} < d < \frac{3c}{2f_1}, \tag{1}$$

where c is the speed of light in a vacuum.

Naturally, the inequality is true if $2f_1 < 3f_0$. Otherwise, it is necessary to focus only on the right side of the inequality and choose d close to $\frac{3c}{2f_1}$, ensuring the operation of the device in the low-frequency range during subsequent modeling steps.

Consider the problem of in-phase excitation of channels 1 and 4. In this case, two incident H_{10} modes of the waveguide with width $d/2$ combine at the slot to form one H_{10} mode of the waveguide with width d. As this mode propagates along the length L, it acquires a phase shift equal to

$$\varphi_1(\lambda) = \frac{2\pi L}{\lambda}\sqrt{1-\left(\frac{\lambda}{2d}\right)^2},$$

where λ is the wavelength in the waveguide.

Next, the resulting mode splits into H_{10} modes in channels 2 and 3. In the case of antiphase excitation of ports 1 and 4, the incident field forms a propagating H_{20} mode, which receives the phase shift equal to

$$\varphi_2(\lambda) = \frac{2\pi L}{\lambda}\sqrt{1-\left(\frac{\lambda}{d}\right)^2}.$$

Subsequently, it splits back into the main modes in channels 2 and 3. For the structure to exhibit quadrature bridge properties, it is necessary that[4] $\varphi_1(\lambda) - \varphi_2(\lambda) = \frac{\pi}{2}$, then

$$L = \frac{\lambda}{4}\frac{1}{\sqrt{1-\left(\frac{\lambda}{2d}\right)^2} - \sqrt{1-\left(\frac{\lambda}{d}\right)^2}}. \quad (2)$$

Thus, by selecting d to satisfy inequality (1) and using formula (2) to determine the value of L for the chosen d, we obtain initial approximations of these geometric parameters for subsequent modeling.

3. In the considered theoretical model, the distance between the waveguides was assumed to be 0, which is impossible from a practical point of view. At this stage of the design, it is necessary to account for the effect of a metal septum between the feeding waveguides (Fig. 1) and determine its minimum allowable width, i.e., the value of parameter e, based on the manufacturing capabilities.

4. In the previous steps 2 and 3, the widths of the feeding waveguides did not match the width a, defined in step 1. The goal of this stage is to integrate the resulting division area with the waveguides of the desired size. To achieve this, it is necessary to determine the initial approximations for the parameters n and s. As shown in Fig. 1, the region described by these parameters is essentially a smooth transition between the rectangular waveguide and the splitting region. The choice of these parameters will be determined not only by the amplitude-frequency characteristics, but also by the further manufacturing process for each specific product, as well as the requirements for the necessary structural strength. For example, the width n should not be too smaller than the diameter of the milling cutter used to fabricate the structure, otherwise the septum may break during manufacture or assembly.

5. At the final stage of modeling, the optimization process should be used to determine the values of the specified geometric parameters. It is convenient to use the following set as an optimization criterion:

$$S_{11},\ S_{41} < \beta;\quad -3dB - \alpha < S_{21},\ S_{31} < -3dB + \alpha,$$

where β is determined based on the requirement for matching the structure and isolation of port 4, while α defines the proximity to equal power division between ports 2 and 3. S_{11} is the amplitude of the reflection coefficient of the main mode in channel 1, and S_{21}, S_{31} and S_{41} are the amplitude of the transmission coefficients of the main mode into ports 2, 3 or 4 when port 1 is excited by the main mode.

It should be noted that the topology in Fig. 1 contains irregularities in the form of corners. Naturally, these irregularities will affect its electromagnetic characteristics. Moreover, in practice, they will be

[4] Vol'man V.I., Pimenov Iu.V. Tekhnicheskaia elektrodinamika [Technical electrodynamics]. Moscow: Sviaz', 1971.

rounded off. Therefore, the corner rounding radii must also be included as optimization parameters. The limiting values of these radii will be determined by the further technological process such as the diameters of the milling cutters used.

Application of the proposed topology and design methodology

The proposed approach to PD design is illustrated using the development of a PD for the 27–35 GHz frequency range.

1. To design a waveguide-slot bridge in the frequency range of 27–35 GHz, a standard WR28 rectangular waveguide with geometric dimensions of 7.11×3.56 mm^2 is used.

2. Using formulas (1) and (2), we obtain that 11.11 mm < d < 12.85 mm. Let us choose d = 11.2 mm, then the L values will be in the range from 9 to 12 mm.

Fig. 3 shows the reflection coefficient for the theoretical model (Fig. 2) at different values of L and the selected d. When choosing initial approximations of geometric parameters, the reflection coefficient S_{11} can be prioritized, as its behavior is generally used to assess the operating band of the device.

As shown in Fig. 3, the best matching from the point of view of the frequency range is achieved at L equal to 10 or 11 mm. Fig. 4 shows the amplitude-frequency characteristics of the transmission coefficients at L = 11 mm.

3. Having set the initial approximations for the parameters d = 11.2 mm and L = 11 m, let's consider how the amplitude-frequency response of the QWSB changes when a non-zero distance appears between the feeding waveguides. With the width of the waveguides fixed at $d/2$, we change e (Fig. 1). In this case, the width of the splitting region increases by the value of e. As seen in Fig. 5, the reflection

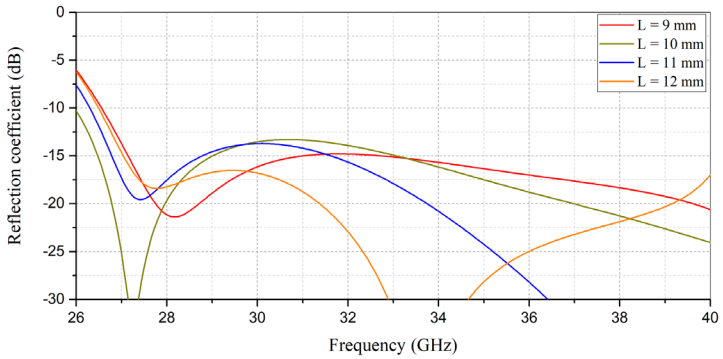

Fig. 3. Reflection coefficient versus frequency with varying L

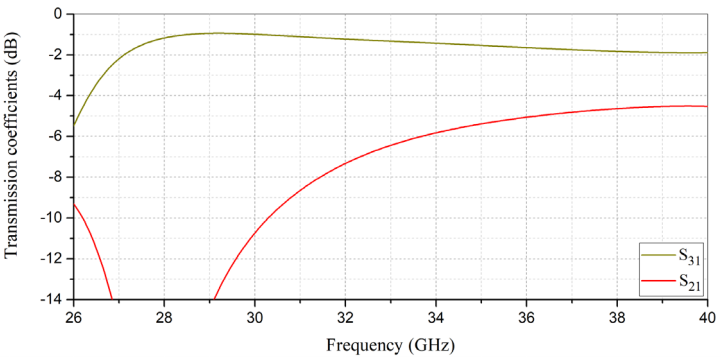

Fig. 4. Transmission coefficients versus frequency at L = 11 mm

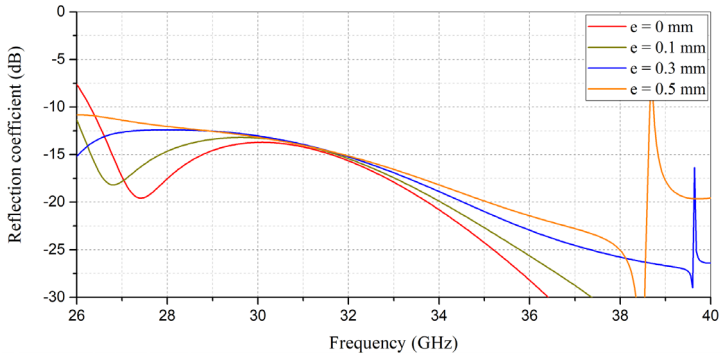

Fig. 5. Reflection coefficient versus frequency with varying e

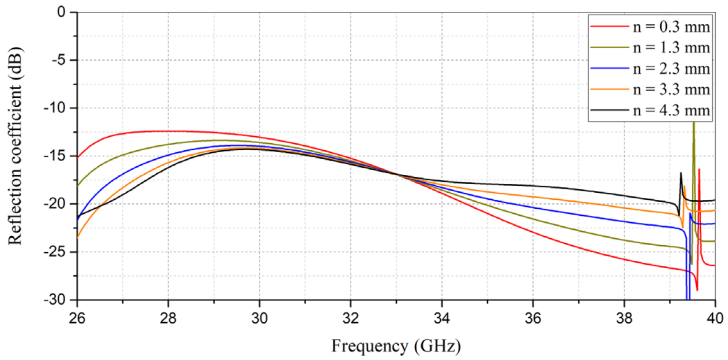

Fig. 6. Reflection coefficient versus frequency with varying n at e = 0.3 mm and s = 10 mm

coefficient S_{11} deteriorates significantly even with a small width of the septum that occurs between the feeding channels and the operating band of the PD shifts to the low-frequency region. This problem can be solved by smoothly increasing the distance between the channels. In this case, the parameter e can be selected relatively small, but not zero. Therefore, for further PD modeling, the value e = 0.3 mm was chosen, at which the obtained reflection coefficient lies in a desired frequency band.

4. Next, we will set the initial approximations for the parameters n and s, which determine smooth transitions between the projected division area and regular WR28 waveguides. Let s = 10 mm, which corresponds to the wavelength of the center of the studied range. Fig. 6 shows that as the parameter n increases, the matching improves and the working bandwidth expands. It should be borne in mind that further increases in n will result in larger weight and size parameters. Therefore, at this stage, we will fix n = 3.3 mm. Fig. 7 illustrates the effect of the transition length on the frequency response of the QWSB. On the one hand, an increase in s reduces the size of the QWSB, while on the other hand, the QWSB model becomes more consistent in the high-frequency range. For further design, the value s = = 5.5 mm was chosen.

The amplitude-frequency characteristics for the selected initial geometric parameters are shown in Fig. 8.

5. Having determined the initial parameters for the proposed topology, the final stage involved searching for optimal parameters. As a result of the optimization process in Ansys HFSS, taking into account the rounding of the corners of the topology, the quadrature PD configuration was obtained that ensures matching S_{11} at least –22 dB with a difference in the amplitudes of the transmission coefficients of the output ports S_{21} and S_{31} not exceeding 0.5 dB and the transmission coefficient S_{41} not exceeding

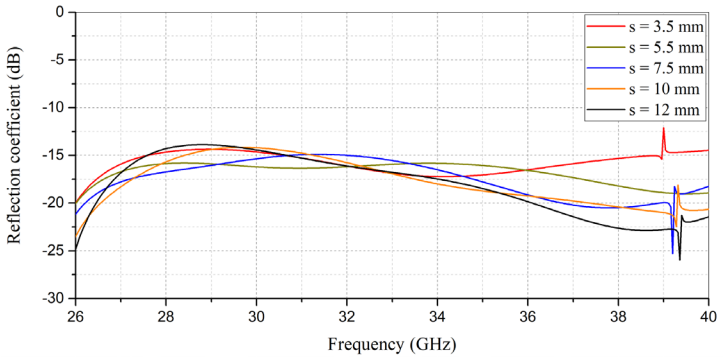

Fig. 7. Reflection coefficient versus frequency with varying *s*

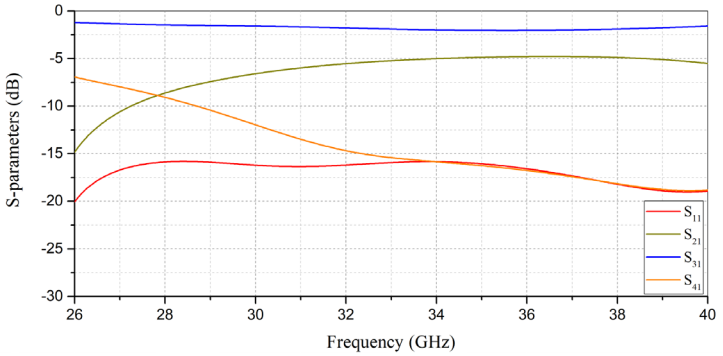

Fig. 8. Amplitude-frequency characteristics for the chosen initial parameters

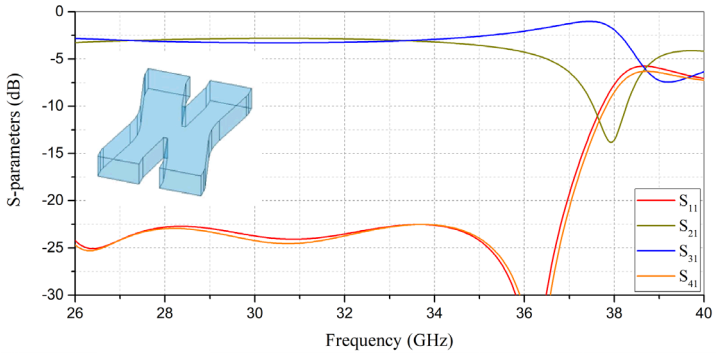

Fig. 9. Amplitude-frequency characteristics at optimal values of the main parameters

–22 dB in a given frequency range. According to the requirements for the quadrature PD, the phase difference between the output ports is 90°. The frequency characteristics of the developed model are shown in Figs. 9 and 10.

The optimal values of the main geometric parameters are shown in Table.

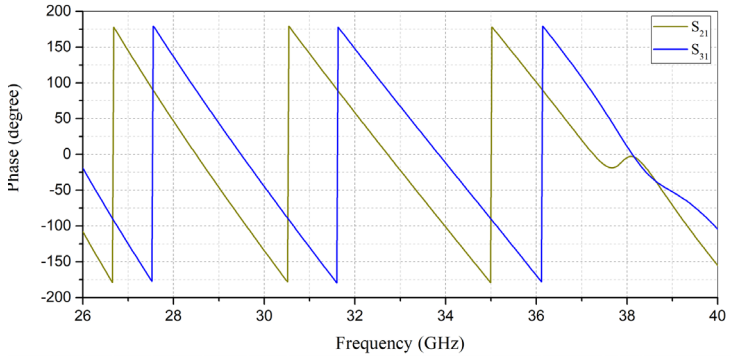

Fig. 10. Dependence of the phases of the output channels on the frequency

Table

Optimal values of the main parameters of the QWSB model

Parameter	Optimal value, mm
d	12.8
e	0.6
L	9.3
n	3.4
s	6.5

Experimental verification of the proposed approach

Based on the obtained model, an experimental sample of a quadrature PD was fabricated (Fig. 11). A matched load was installed in port 4 of the PD. A vector network analyzer was used to measure the frequency characteristics. The analyzer's measurement cables and the waveguide ports of the quadrature bridge were connected via pre-calibrated coaxial waveguide junctions. Each of the output ports was examined separately (Fig. 12).

A comparison of the experimental and calculated curves in Fig. 13 shows a high degree of correspondence in the required frequency range of 27–35 GHz. The shapes of the curves for the reflection coefficient (Fig. 13, *a*) and the transmission coefficients (Fig. 13, *b*) demonstrate similar characteristics and quantitative values, which confirms the accuracy of the simulation. Although the experimental

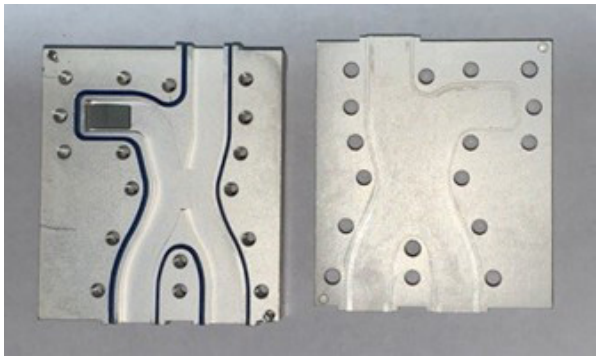

Fig. 11. Experimental sample of a quadrature PD

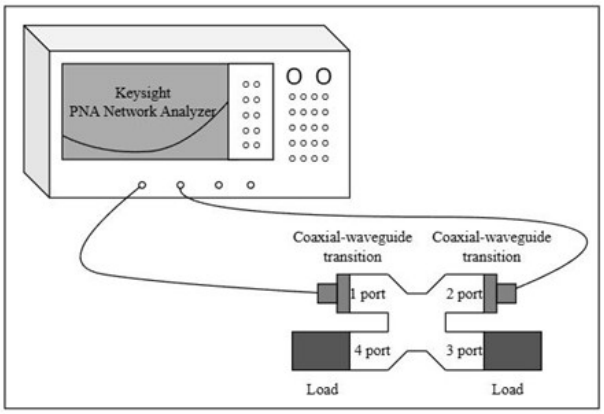

Fig. 12. Experimental setup for measuring a quadrature PD

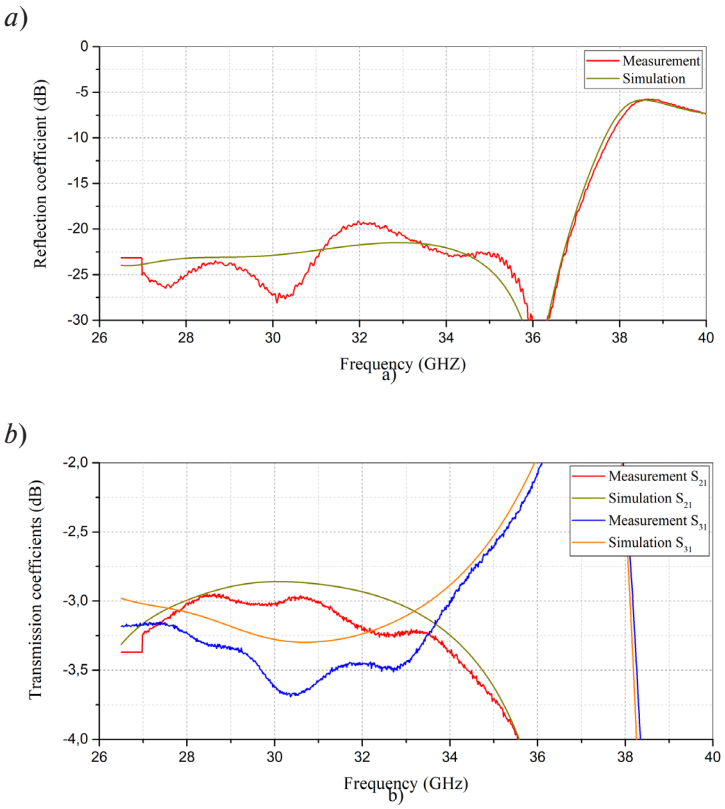

Fig. 13. Dependences of calculated and measured S_{11} on frequency (*a*); dependences of calculated and measured S_{21} and S_{31} on frequency (*b*)

curves have a more resonant character, this is explained by the measurement methodology and the use of matched loads in ports. Outside the division range, there is an almost complete coincidence of the curves, which indicates the reliability of the computational model in a wider frequency range. It should be noted that a discrepancy between the measured and simulated results can be also attributed to the roughness of the inner surfaces of the quadrature PD. Polishing these surfaces reduces losses, which would bring the experimental curves even closer to the calculated ones, as also discussed in [14, 15].

Conclusion

The topology of a quadrature waveguide PD and its design methodology have been developed, which makes it possible to create a PD for a predefined frequency range. The proposed approach is demonstrated by modeling an H-plane PD for operation in the frequency range of 27–35 GHz. The obtained model was verified by manufacturing a prototype and measuring its frequency characteristics. The measurement results confirmed the agreement between the calculated data and the real characteristics, thereby validating the proposed approach.

REFERENCES

1. **Sakata S., Komatsuzaki Y., Shinjo S.** Adaptive input-power distribution in Doherty power amplifier using modified Wilkinson power divider. *2020 IEEE Topical Conference on RF/Microwave Power Amplifiers for Radio and Wireless Applications* (*PAWR*), 2020, Pp. 34–37. DOI: 10.1109/PAWR46754.2020.9036005

2. **Romodin V.B., Kulik V.S.** Microstrip divider for compactsynthetic aperture radar antenna array. *Interekspo Geo-Sibir'*, 2017.

3. **Zhai G., Shi B.** Compact low loss millimeter wave 8-way radial waveguide power combiner. *TENCON 2017 – 2017 IEEE Region 10 Conference*, 2017, Pp. 1598–1601. DOI: 10.1109/TENCON.2017.8228112

4. **Abramson O., Gabbay D., Sharon A.** Applications of RF-over-fiber technology in the defense and civilian markets. *Microwave Journal, June Supplement*, 2025, P. 6.

5. **Park S.** Beyond copper and optical, a new interconnect eyes next gen data centers. *All About Circuits*, 2025.

6. **Mozharovskiy A.V., Soykin O.V., Artemenko A.A., Maslennikov R.O., Vendik I.B.** Wideband waveguide-to-microstrip transition for mm-wave applications. *Journal of the Russian Universities. Radioelectronics*, 2019, Vol. 22, No. 5, Pp. 17–32. DOI: 10.32603/1993-8985-2019-22-5-17-32

7. **Zhang L., Liu T.** A new H-plane T-junction waveguide power divider covering the full W-band. *2020 IEEE 3rd International Conference on Electronic Information and Communication Technology* (*ICEICT*), 2020, Pp. 803–805. DOI: 10.1109/ICEICT51264.2020.9334336

8. **Zhao P., Wang Q., Zhang F., He X.** A novel T-junction waveguide power divider with anti-phases and broad bandwidth. *2017 IEEE International Symposium on Antennas and Propagation & USNC/URSI National Radio Science Meeting*, 2017, Pp. 741–742. DOI: 10.1109/APUSNCURSINRSM.2017.8072413

9. **Deng J., Wang Q., Zhao P., Tian M., Li Q.** A quasi-planar H-Plane waveguide power divider with full bandwidth. *IEEE Microwave and Wireless Components Letters*, 2018, Vol. 28, No. 8, Pp. 645–647. DOI: 10.1109/LMWC.2018.2847028

10. **Zheng P., Zhou P., Yu W.-H., Sun H.-J., Lv X., Deng H.** W-band power divider based on H-plane slot waveguide bridge. *2012 International Conference on Microwave and Millimeter Wave Technology* (*ICMMT*), 2012, Pp. 1–4. DOI: 10.1109/ICMMT.2012.6230025

11. **Kang Y., Lin X.Q., Fan Y.** A THz one-to-four power divider with high isolation and arbitrary phase shift. *2020 International Conference on Microwave and Millimeter Wave Technology* (*ICMMT*), 2020, Pp. 1–3. DOI: 10.1109/ICMMT49418.2020.9386897

12. **Epp L.W., Hoppe D.J., Khan A.R., Stride S.L.** A high-power *Ka*-Band (31–36 GHz) solid-state amplifier based on low-loss corporate waveguide combining. *IEEE Transactions on Microwave Theory and Techniques*, 2008, Vol. 56, No. 8, Pp. 1899–1908. DOI: 10.1109/TMTT.2008.927299

13. **Hildebrand L.T.** Results for a simple compact narrow-wall directional coupler. *IEEE Microwave and Guided Wave Letters*, 2000, Vol. 10, No. 6, Pp. 231–232. DOI: 10.1109/75.852425

14. **Wang R., Cui W.** A rapid estimation of the conductor loss in the rectangular waveguide with rough surface. *2011 4th IEEE International Symposium on Microwave, Antenna, Propagation and EMC Technologies for Wireless Communications*, 2011, Pp. 498–500. DOI: 10.1109/MAPE.2011.6156144

15. **Hofmann A., Lomakin K., Kleinlein M., Bader T., Sippel M., Gold G.** SLS-printed E-band waveguides and the impact of surface roughness. *2023 53rd European Microwave Conference* (*EuMC*), 2023, Pp. 243–246. DOI: 10.23919/EuMC58039.2023.10290537

INFORMATION ABOUT AUTHORS / СВЕДЕНИЯ ОБ АВТОРАХ

Dzhuletta V. Lomsadze
Ломсадзе Джульетта Васильевна
E-mail: dlomsadze31@yandex.ru

Natalia G. Kolmakova
Колмакова Наталья Геннадьевна
E-mail: kolmakova.nataliya@gmail.com
ORCID: https://orcid.org/0000-0003-2595-4903

Sergey V. Volvenko
Волвенко Сергей Валентинович
E-mail: volk@cee.spbstu.ru
ORCID: https://orcid.org/0000-0001-7726-8492

Submitted: 05.06.2025; Approved: 11.09.2025; Accepted: 22.09.2025.
Поступила: 05.06.2025; Одобрена: 11.09.2025; Принята: 22.09.2025.